Algal Research 95 (2026) 104626

Contents lists available at ScienceDirect

Algal Research

journal homepage: www.elsevier.com/locate/algal

Hyperproduction of lutein and protein in a novel yellow mutant of *Chlorella sorokiniana* via modulation of carbon-nitrogen metabolism under high-cell-density heterotrophic cultivation

Yucheng Chen [a,c,d], Zehao Qiu [a,c,d], Wen Zhang [a,c,d], Xinxin Huang [a,c,d], Ruijuan Ma [b,*], Baobei Wang [e], Shih-Hsin Ho [c,f], Jianfeng Chen [a,c,d], Youping Xie [a,c,d,**]

[a] *Marine Biological Manufacturing Center of Fuzhou Institute of Oceanography, Fuzhou University, Fuzhou, 350108, China*
[b] *State Key Laboratory for Mariculture Breeding, Fisheries College, Jimei University, Xiamen, Fujian, 361021, China*
[c] *Fujian Engineering and Technology Research Center for Comprehensive Utilization of Marine Products Waste, Fuzhou University, Fuzhou, 350108, China*
[d] *Fuzhou Industrial Technology Innovation Center for High Value Utilization of Marine Products, Fuzhou University, Fuzhou, 350108, China*
[e] *Fujian Province Key Laboratory for the Development of Bioactive Material from Marine Algae, Quanzhou Normal University, Quanzhou, 362000, China*
[f] *State Key Laboratory of Urban Water Resource and Environment, School of Environment, Harbin Institute of Technology, Harbin, 150090, China*

ARTICLE INFO

Keywords:
Chlorella sorokiniana
Heterotrophic cultivation
Carbon-nitrogen metabolism
Lutein synthesis
Protein synthesis

ABSTRACT

Chlorella sorokiniana is capable of high-cell-density heterotrophic cultivation, endowing it with exceptional potential for large-scale, efficient lutein production. However, its industrial application has been hindered by low lutein content and the inability to precisely control carotenoid composition. To address these limitations, a chlorophyll-deficient and lutein-enriched yellow mutant *C. sorokiniana* MT03 was employed to investigate the effects of carbon–nitrogen (C/N) ratio modulation on lutein and protein production under heterotrophic conditions. Systematic optimization identified a C/N ratio of 16 as optimal, resulting in marked enhancement of both lutein and protein accumulation. Integrated physiological and transcriptomic analyses demonstrated that carbon depletion combined with nitrogen repletion coordinately regulated central carbon metabolism, macromolecular biosynthesis, heme homeostasis, and carotenoid biosynthetic pathways. Notably, key genes involved in fatty acid biosynthesis, starch degradation, amino acid biosynthesis, and carotenoid formation were significantly upregulated, highlighting the tight integration of nitrogen availability with carbon partitioning. Heme accumulation was found to enhance CYP97-mediated lutein synthesis, further linking nitrogen status to carotenogenic flux. A two-stage cultivation strategy, comprising (I) fed-batch growth for high-cell-density biomass production, followed by (II) carbon-depleted and nitrogen-replete conditions to trigger lutein and protein synthesis, was successfully implemented in a 5-L bioreactor. This approach yielded a final biomass concentration of 184.46 g/L, with volumetric titers of 481.63 mg/L lutein and 76.31 g/L protein, surpassing most values reported in the literature. These results demonstrate that rational C/N metabolic regulation effectively redirects carbon flux toward target metabolites, providing a scalable and industrially viable platform for the co-production of lutein and protein in microalgae.

1. Introduction

Lutein is a major constituent of macular pigment in the human retina and exhibits potent antioxidant, anti-inflammatory, and natural coloring properties, leading to its extensive application in animal feed, food formulations, and pharmaceutical products [1–3]. Currently, commercial lutein is predominantly extracted from marigold; however, this approach is constrained by high operational costs and susceptibility to seasonal and climatic fluctuations, which hinder its sustainable development and broader application [1]. Although microbial platforms for fermentative lutein production are promising, the lengthy biosynthetic pathway, particularly the asymmetric cyclization and hydroxylation steps, poses significant challenges, including low yields, byproduct accumulation, and complex metabolic regulation [4,5]. In contrast,

* Corresponding author.
** Correspondence to: Y. Xie, Marine Biological Manufacturing Center of Fuzhou Institute of Oceanography, Fuzhou University, Fuzhou, 350108, China.
E-mail addresses: rjma@jmu.edu.cn (R. Ma), ypxie@fzu.edu.cn (Y. Xie).

https://doi.org/10.1016/j.algal.2026.104626
Received 2 December 2025; Received in revised form 15 February 2026; Accepted 28 February 2026
Available online 3 March 2026

microalgae naturally possess a complete lutein biosynthetic pathway and combine rapid growth with inherently high lutein content, positioning them as the most promising sustainable platform for natural lutein production [6,7].

Chlorella is a commercially promising strain that has been extensively studied worldwide [8,9]. Conventional commercial *Chlorella* cultivation relies primarily on the photoautotrophic mode, which is inherently constrained by limited light penetration and cell shading effects, thereby hindering high-cell-density cultivation and, consequently, high lutein production. Heterotrophic cultivation, by contrast, represents a more industrially viable strategy, as it enables rapid algal proliferation driven by organic carbon sources, facilitating high biomass accumulation within a short timeframe and offering a scalable route for high-value metabolite production. Notably, recent studies have shown that *Chlorella sorokiniana* can achieve ultrahigh-density heterotrophic cultures (dry cell weight $>$ 200 g/L), highlighting its exceptional potential for industrial-scale bioproduction [10,11]. However, a critical bottleneck remains: under heterotrophic conditions, the lutein content in *C. sorokiniana* (1.73–3.75 mg/g DCW) is substantially lower than that observed under photoautotrophic or mixotrophic modes (6.16–17.4 mg/g DCW) [12–19]. Although two-stage strategies combining heterotrophic growth followed by photoautotrophic or mixotrophic induction have been explored to enhance lutein accumulation [15,20], such approaches require system switching, cell dilution, and light exposure, thereby increasing process complexity, energy consumption, and operational costs while compromising production continuity and economic feasibility. Moreover, under heterotrophic conditions, algal cells continue to synthesize chlorophyll and other carotenoids, such as violaxanthin, neoxanthin, and β-carotene [12]. Chlorophyll and carotenoids both originate from the common precursor geranylgeranyl pyrophosphate (GGPP) [21]. Meanwhile, other carotenoids, such as violaxanthin, neoxanthin, and β-carotene, diverge biosynthetically from lutein, with lycopene serving as their shared precursor [22]. Hence, chlorophyll and other carotenoids compete with lutein for shared metabolic precursors. These co-produced pigments also introduce impurities during downstream extraction and purification, further complicating separation and elevating processing costs [23].

The ethyl methanesulfonate (EMS)-derived yellow mutant *C. sorokiniana* MT03 exhibits a chlorophyll-deficient phenotype coupled with enhanced lutein accumulation under heterotrophic conditions, resulting in lutein becoming the dominant intracellular pigment [24]. Nevertheless, lutein content in this strain remains suboptimal under heterotrophy, and effective strategies to achieve high-level lutein accumulation are still lacking. Modulating the carbon-to-nitrogen (C/N) ratio offers a simple yet highly effective strategy to enhance metabolite accumulation and boost both titer and productivity in microalgal systems. For instance, in heterotrophic cultures of *Chlorella* sp. MBFJNU-17, shifting the C/N ratio from 40 (40 g/L glucose, 1 g/L urea) in the growth phase to 1.7 (5 g/L glucose, 3 g/L urea) in the production phase successfully redirected intracellular starch toward protein synthesis, achieving a protein content of 59.75% [25]. Similarly, in *C. sorokiniana* CMBB276, a two-stage nitrogen feeding approach involving a reduction of the C/N ratio from 18 to 6 concurrently enhances both protein content and volumetric titer, resulting in a peak protein content of 58.6% (*w*/w) and a final titer of 87.0 g/L [26]. Given that lutein in microalgal cells primarily binds to light-harvesting complex proteins, its biosynthesis is often coordinated with protein production [27]. This co-regulation suggests that strategic modulation of carbon–nitrogen metabolism may concurrently enhance both lutein and protein accumulation in heterotrophically grown microalgae.

In this study, the yellow mutant *C. sorokiniana* MT03 was employed as a model system to evaluate how varying C/N ratios influence cell growth, nutrient utilization, and cellular composition. Integrated transcriptomic analyses were conducted to uncover the molecular mechanisms governing C/N-mediated regulation of lutein and protein biosynthesis. The efficacy of the developed C/N ratio-based metabolic strategy was further validated in a 5-L bioreactor under controlled fed-batch cultivation conditions. The results provide a rational and scalable framework to address the key technical bottleneck currently impeding the industrial-scale production of microalgal lutein and protein.

2. Materials and methods

2.1. Microalgal strain and seed culture

The yellow mutant *C. sorokiniana* MT03, developed via EMS mutagenesis [24], was stored at −80 °C in 15% (*v*/v) glycerol. Upon thawing, 50 μL aliquots of the algal stock were spread onto solidified modified Mann and Myer's (MM) medium [12] and incubated in the dark at 30 °C. After 7 days, algal colonies were inoculated into 100 mL of liquid MM medium in 250 mL Erlenmeyer flasks and cultivated for 3 days at 30 °C and 150 rpm to generate seed cultures.

2.2. Cultivation of MT03 under different carbon-nitrogen ratios

A 100 mL volume of fresh medium in a 250 mL Erlenmeyer flask was inoculated with the seed culture to achieve an algal cell density of 0.15 g/L. A fixed glucose concentration of 10 g/L was used in the fresh medium, with sodium nitrate varied at 0.5, 1.75, and 3.0 g/L to establish C/N molar ratios of 57:1, 16:1, and 9:1, respectively. Cultures were incubated in the dark on an orbital shaker at 30 °C and 200 rpm, to ensure sufficient oxygen supply. Following complete glucose depletion, cultivation was continued for an additional three days to monitor post-depletion physiological responses. Throughout the experiment, biomass accumulation and nutrient consumption were tracked at regular intervals. Sampling time points were designated as GD-1, GD, GD+1, GD+2, and GD+3, corresponding to one day prior to glucose depletion, the day of glucose depletion, one, two-, and three-days post-glucose depletion, respectively. The experiments were conducted concurrently with our previous work [24], sharing the data of the group with a C/N molar ratio of 16:1 but for distinct analytical objectives.

2.3. Cultivation of MT03 in a 5-L bioreactor

The seed culture was transferred into a 5-L stirred-tank bioreactor (T&J-Atype 5 L, T&J Bio-engineering Co. LTD., Shanghai, China) containing 2.5 L of optimized Mann and Myer's medium, formulated as follows (per liter): 26 g glucose, 0.8 g $MgSO_4{\cdot}7H_2O$, 1.62 g urea, 0.2 g $CaCl_2{\cdot}2H_2O$, 0.4 g $K_2HPO_4{\cdot}3H_2O$, 0.15 g EDTA·2Na, 30 mg H_3BO_3, 30 mg $FeSO_4{\cdot}7H_2O$, 7 mg $MnCl_2{\cdot}4H_2O$, 1.65 mg $ZnSO_4{\cdot}7H_2O$, 0.035 mg $Co(NO_3)_2{\cdot}6H_2O$, and 0.01 mg $CuSO_4{\cdot}5H_2O$. The substitution of sodium nitrate with urea as the nitrogen source is intended to avoid the need for substantial acid or alkali supplementation to maintain a stable pH, thereby preventing the accumulation of high salt levels, such as sodium chloride, that could subsequently inhibit cell growth [10]. The initial cell density in the bioreactor was 1.4 g/L. Cultivation was carried out at 30 °C with an agitation speed of 200 rpm and an aeration rate of 1.0 vvm. The pH was controlled at 6.8 through automated dosing of 4 mol/L NaOH or 1 mol/L H_2SO_4 as required. To ensure adequate oxygen supply, the agitation speed was dynamically increased whenever the dissolved oxygen (DO) concentration fell below 20% air saturation, thereby maintaining DO at approximately 20%. Throughout the fermentation, glucose was kept at ~5 g/L by fed-batch addition of a 22.85-fold concentrated medium via a peristaltic pump. To ensure precise control of glucose concentration, frequent offline sampling was conducted to quantify residual glucose in the culture broth, and the pump flow rate was manually adjusted based on these measurements. The dynamic profile of flow rate adjustments during the fermentation is detailed in Fig. S1. Feeding was terminated once the biomass concentration exceeded 200 g/L, thereby establishing carbon-depleted but nitrogen-replete conditions for an additional 48-h induction phase. Biomass and residual nitrogen source concentrations were quantified every 12 h.

Algal cells were harvested daily by centrifugation, followed by immediate freeze-dried and stored at −80 °C until further analysis of lutein and protein contents.

2.4. Characterization of algal growth and intracellular composition

Biomass concentration was determined as dry cell weight (DCW) following a published protocol [12]. Glucose, nitrogen, and carotenoid levels were quantified using established methods from the same study. Carbohydrate content was assessed via a modified quantitative saccharification approach [28], while total lipids were measured using a direct transesterification procedure [29]. Protein extraction and amino acid composition analysis were performed following procedures detailed in an earlier study [30].

Heme extraction and quantification followed a published protocol with minor modifications [31]. Briefly, 100 mg of dried biomass was homogenized in a cryogenic grinder (JXFSTPRP-CLN, Shanghai Jingxin Industrial Development Co., Ltd., China) with 1 mL of ice-cold acetone/0.1 M NH_4OH (9:1, *v*/v) and 0.5 g of glass beads at 4 °C. The homogenate was centrifuged at 5000 rpm for 5 min, and the supernatant was discarded. This wash was repeated until the pellet appeared white and the supernatant was colorless, indicating complete removal of pigments. Heme was then extracted by resuspending the pellet in 1 mL of acetone/HCl/dimethyl sulfoxide (10:0.5:2, *v*/v/v) at 4 °C. The resulting extract was analyzed by high-performance liquid chromatography (HPLC; LC-20A, Shimadzu, Japan) equipped with a Poroshell 120 EC-C18 column (100 mm × 3.0 mm, 2.7 μm particle size). The column was maintained at 30 °C with a flow rate of 0.3 mL/min. Mobile phase A consisted of water acidified to pH 3.2 with trifluoroacetic acid, and mobile phase B was methanol. Elution was performed using the following gradient program: 30% B (0–1 min), linear increase to 100% B (1–20 min), hold at 100% B (20–35 min), return to 30% B (35–45 min), and re-equilibration at 30% B (45–75 min). Heme was detected at 398 nm and quantified by a calibration curve generated using haemin (Sigma-Aldrich) as an external standard.

2.5. Transcriptomic analysis

For transcriptomic analysis, samples were collected from flask cultures grown under a C/N ratio of 16:1 at three defined time points: at the moment of glucose depletion (designated M0h), 6 h post-depletion (M6h), and 12 h post-depletion (M12h). Total RNA isolation, cDNA library construction, high-throughput sequencing, and downstream assembly and functional annotation were carried out following the established protocols [32]. Differential expression analysis between M0h versus M6h and M0h versus M12h was identified using both DESeq2 [33] and edgeR [34]. A gene was classified as differentially expressed if it met the following criteria: a false discovery rate (FDR) < 0.05 and an absolute $\log_2$(fold change) > 1. The $\log_2$(fold change) and FDR values for genes involved in carotenoid biosynthesis, porphyrin metabolism, central carbon metabolism, amino acid and fatty acid biosynthesis, starch degradation and synthesis are reported in this study (Table S1 in the supplementary file).

2.6. Statistical analysis

All experiments were performed in biological triplicate. Results for algal growth, nutrient uptake, and biochemical content are expressed as mean ± standard deviation (SD). Significant differences in amino acid composition between M6h/M12h and M0h were assessed using two-tailed Student's *t*-tests, with significance defined as $p < 0.05$ (*) or $p < 0.01$ (**).

3. Results and discussions

3.1. Effect of different carbon-nitrogen ratios on algal growth and nutrient utilization

As illustrated in Fig. 1(a), when the carbon-to-nitrogen (C/N) ratio was set to 57:1, sodium nitrate was completely depleted by day 2, while glucose was exhausted by day 9. During this period, MT03 exhibited steady growth, reaching a maximum biomass concentration of 5.61 g/L upon glucose depletion, after which the biomass slightly declined and stabilized. Notably, following sodium nitrate exhaustion, the glucose consumption rate markedly decreased, and the growth phase was significantly prolonged—likely due to nitrogen limitation, which impaired glucose uptake and consequently suppressed cell proliferation. In contrast, as shown in Fig. 1(b) and (c), when the C/N ratios were adjusted to 16:1 and 9:1, glucose was fully consumed by day 4, yielding maximum biomass concentrations of 5.84 and 5.81 g/L, respectively. Subsequently, biomass levels initially decreased before stabilizing. Compared to the C/N ratio of 57:1, these lower C/N ratios enabled more rapid glucose utilization.

Despite variations in the C/N ratio, the peak biomass concentration of MT03 remained relatively consistent across conditions. These results indicate that, under heterotrophic cultivation, biomass accumulation is primarily governed by glucose availability. This observation aligns with previous studies. For instance, the optimal C/N ratio for *C. sorokiniana* GT-1 growth was identified as 16, whereas further lowering the ratio to 8 showed no significant effect on either biomass yield or glucose consumption [10]. Similarly, *C. sorokiniana* CMBB276 achieved higher biomass at a C/N ratio of 18 compared to ratios of 6, 12, or 24 [11]. Additionally, in all three groups with varying C/N ratios, biomass exhibited a decline trend upon glucose depletion, followed by a stabilization. These results are consistent with the previous study in *C. sorokiniana* GT-1 [10], further confirming the essential role of glucose availability in biomass accumulation. The reason for this phenomenon could be that, upon glucose depletion, microalgal cells experience carbon starvation, potentially leading to cellular damage or death and a corresponding decline in biomass concentration. Consequently, intracellular carbon reserves, such as starch (a short-term energy reserve [35]), may be rapidly degraded into glucose to provide energy for sustaining cell viability, resulting in a relatively stable biomass concentration thereafter. Considering both biomass concentration and nutrient utilization efficiency, a C/N ratio of 16 was identified as optimal for the heterotrophic cultivation of MT03.

3.2. Effect of different carbon-nitrogen ratios on lutein content and cell composition

As shown in Fig. 2(a), under three heterotrophic conditions with varying C/N ratios, the lutein content of MT03 peaked on the third day after carbon depletion (GD+3). Among all culture conditions, the highest lutein content was observed at a C/N ratio of 16:1, reaching 4.34 mg/g DCW. The second-highest content (4.24 mg/g DCW) was achieved at a C/N ratio of 9:1, whereas the maximum lutein content under a C/N ratio of 57:1 was only 1.37 mg/g DCW. These results align with previous reports indicating that lower C/N ratios favor enhanced lutein accumulation in microalgae [19]. For instance, heterotrophic cultivation of *C. sorokiniana* at a C/N ratio of 20 yielded significantly higher lutein content than at a ratio of 60 [36]. These findings collectively indicate that, under heterotrophic conditions, the presence of glucose is unfavorable for lutein biosynthesis in algae, and lutein synthesis is enhanced under glucose-depleted conditions coupled with the maintenance of an adequate nitrogen supply.

As illustrated in Fig. 2(b–d), under varying C/N ratios (57:1, 16:1, and 9:1), the protein content of MT03 progressively increased following carbon depletion, reaching maxima on day 1 (GD+1), 2 (GD+2), and 3 (GD+3) at 279.33, 385.31, and 318.28 mg/g DCW, respectively.

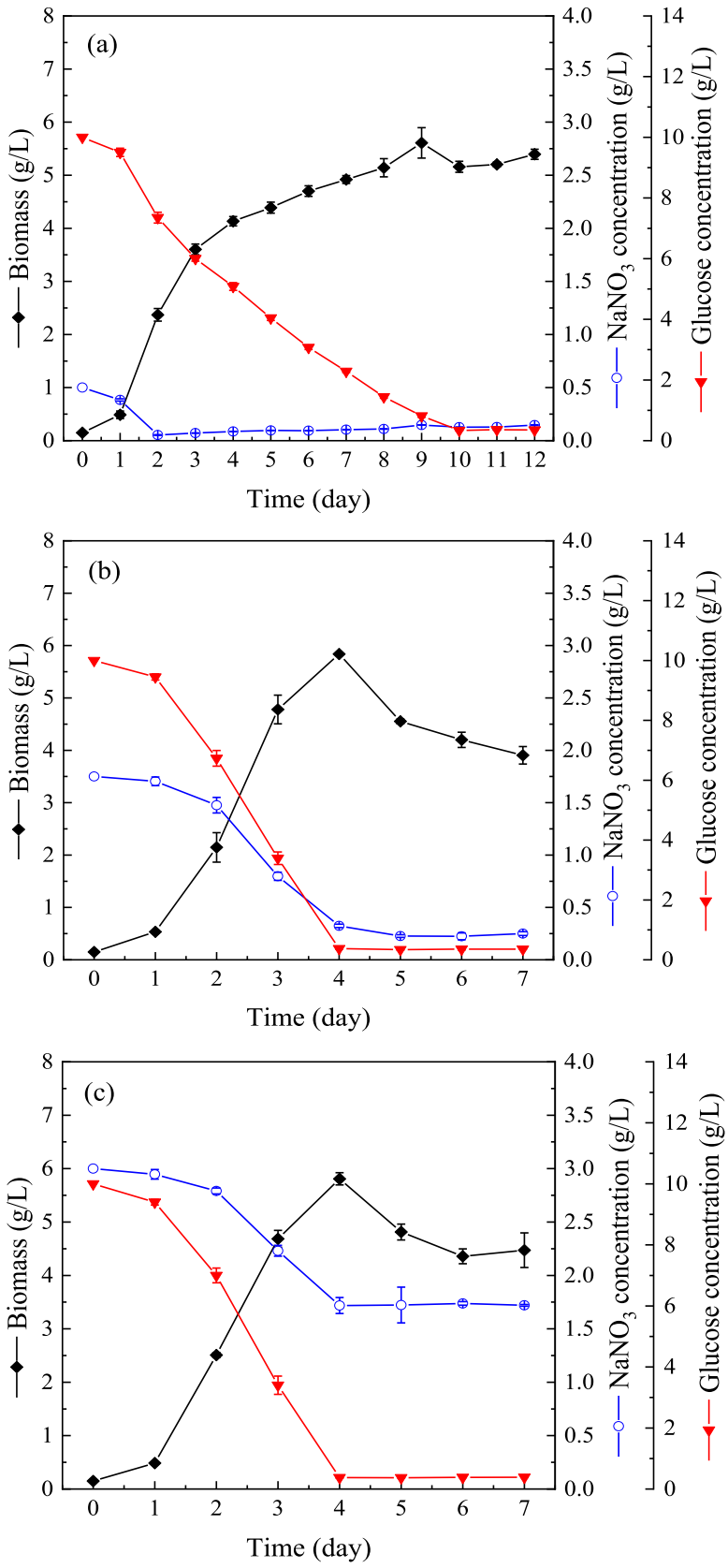

Fig. 1. Time-course profiles of cell growth and nutrient consumption of MT03 cultivated under heterotrophic conditions with varying C/N ratios: (a) 57:1, (b) 16:1, and (c) 9:1. The data of the group with a C/N molar ratio of 16:1 were the same as our previous work [24], due to that the experiments were conducted concurrently, but for distinct analytical objectives.

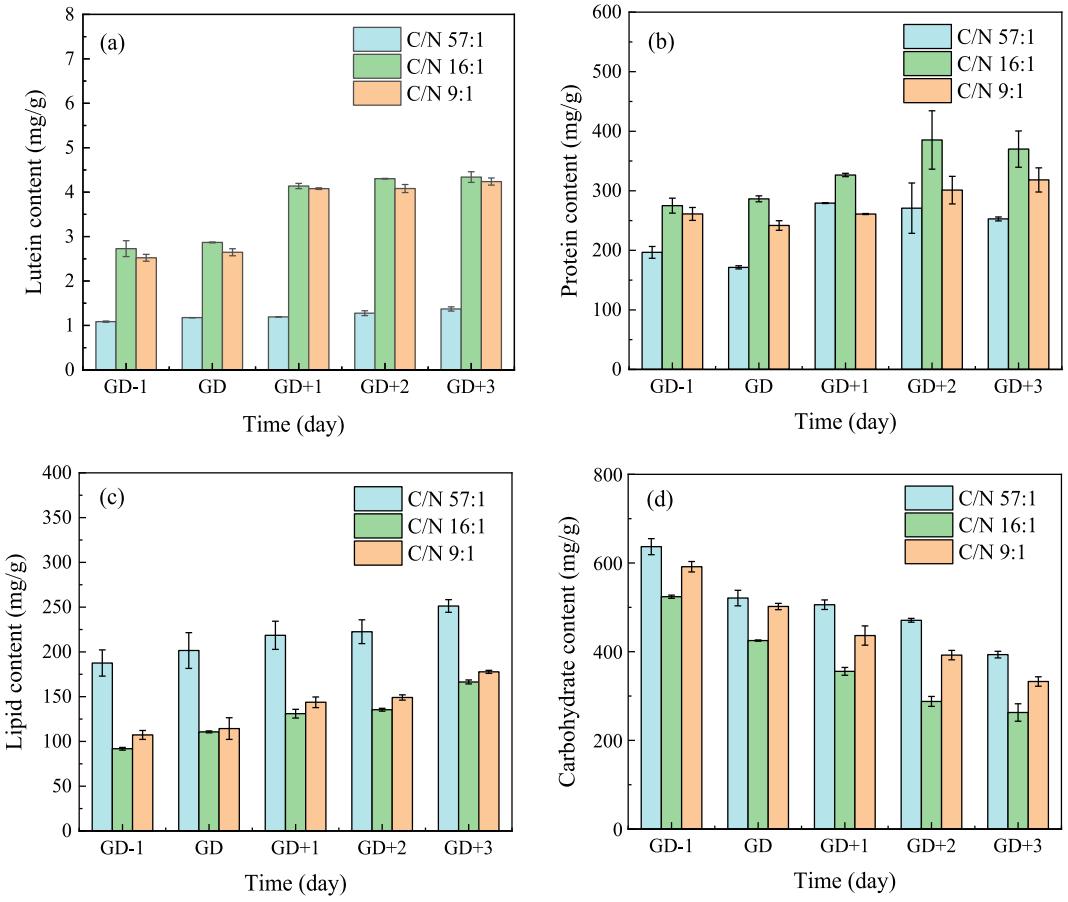

Fig. 2. Temporal dynamics of cellular composition in MT03 under varying C/N ratios, including (a) lutein, (b) protein, (c) lipid, and (d) carbohydrate contents. Time points are defined as follows: GD-1 (one day before glucose depletion), GD (day of glucose depletion), GD+1, GD+2, and GD+3 (one, two, and three days after glucose depletion, respectively). The data of the group with a C/N molar ratio of 16:1 were the same as our previous work [24], due to that the experiments were conducted concurrently, but for distinct analytical objectives.

Concurrently, lipid content exhibited a steady rise throughout the carbon-depleted cultivation period, attaining levels of 251.29, 166.46, and 177.75 mg/g DCW by GD+3 under the respective C/N conditions. In stark contrast, carbohydrate content declined markedly across all treatments, decreasing to 393.45, 262.87, and 332.82 mg/g DCW by GD+3. These findings underscore the profound influence of the C/N ratio on the metabolic reprogramming of *C. sorokiniana*. A previous study has shown that under heterotrophic cultivation with organic carbon supplementation, rapidly proliferating algal cells tend to accumulate substantial carbohydrate reserves [10]. Consistently, before carbon depletion, MT03 cells typically contained carbohydrates exceeding 50% of their dry cell weight (DCW). Furthermore, cultures grown under high C/N ratios (e.g., 57:1) accumulated relatively higher levels of both lipids and carbohydrates but exhibited lower protein content. Notably, the lipid content at a C/N ratio of 57:1 was substantially higher than that observed under the lower C/N ratios (16:1 and 9:1), likely due to nitrogen limitation, which redirects carbon flux toward the synthesis of energy-dense storage compounds as an adaptive strategy under nutrient imbalance [37]. Upon carbon depletion, algal cells appear to catabolize endogenous carbohydrates to maintain a carbon supply for essential biosynthetic processes, including the production of proteins and energy-rich lipids necessary for cellular maintenance and survival. Under these conditions, the availability of intracellular nitrogen reserves or external nitrogen sources plays a pivotal role in facilitating enhanced protein synthesis. This metabolic shift aligns with observations in other microalgal systems. For instance, during the second-stage cultivation of *Chlorella* sp. MBFJNU-17 under a low C/N ratio (1.5), intracellular starch content plummeted from ~55% to 15% following glucose exhaustion, concomitant with a sharp increase in protein content from 19.45% to 63.48% [25].

Together, these results highlight the dynamic interplay between carbon and nitrogen availability in regulating macromolecular partitioning in microalgae. In particular, the increased co-synthesis of lutein and protein under carbon-depleted and nitrogen-replete conditions suggests the feasibility of a two-stage cultivation strategy. This approach would involve supplying sufficient carbon and nitrogen in the first stage to achieve high biomass concentration, followed by a second stage under carbon depletion and nitrogen repletion to promote the accumulation of lutein and protein. Such a strategy may be applicable not only to other strains of *C. sorokiniana*, but also potentially to other microalgae species.

3.3. *Transcriptomic insights into regulatory mechanisms of carbon–nitrogen metabolism*

To further elucidate the molecular mechanisms underlying the elevated lutein and protein contents in MT03 under a C/N ratio of 16:1, particularly in light of their pronounced accumulation following carbon depletion, comprehensive transcriptomic analyses were conducted at three time points: the onset of carbon depletion (M0h), 6 h post-depletion (M6h), and 12 h post-depletion (M12h). As illustrated in Fig. 3(a), clear separation among samples collected at M0h, M6h, and M12h along PC1 indicates substantial transcriptional reprogramming in response to carbon depletion. Differential gene expression (DEG) analysis revealed that, compared with M0h, 253 genes were significantly upregulated and 844 were downregulated at M6h (Fig. 3(b)). In the comparison between M12h and M0h, the number of DEGs increased

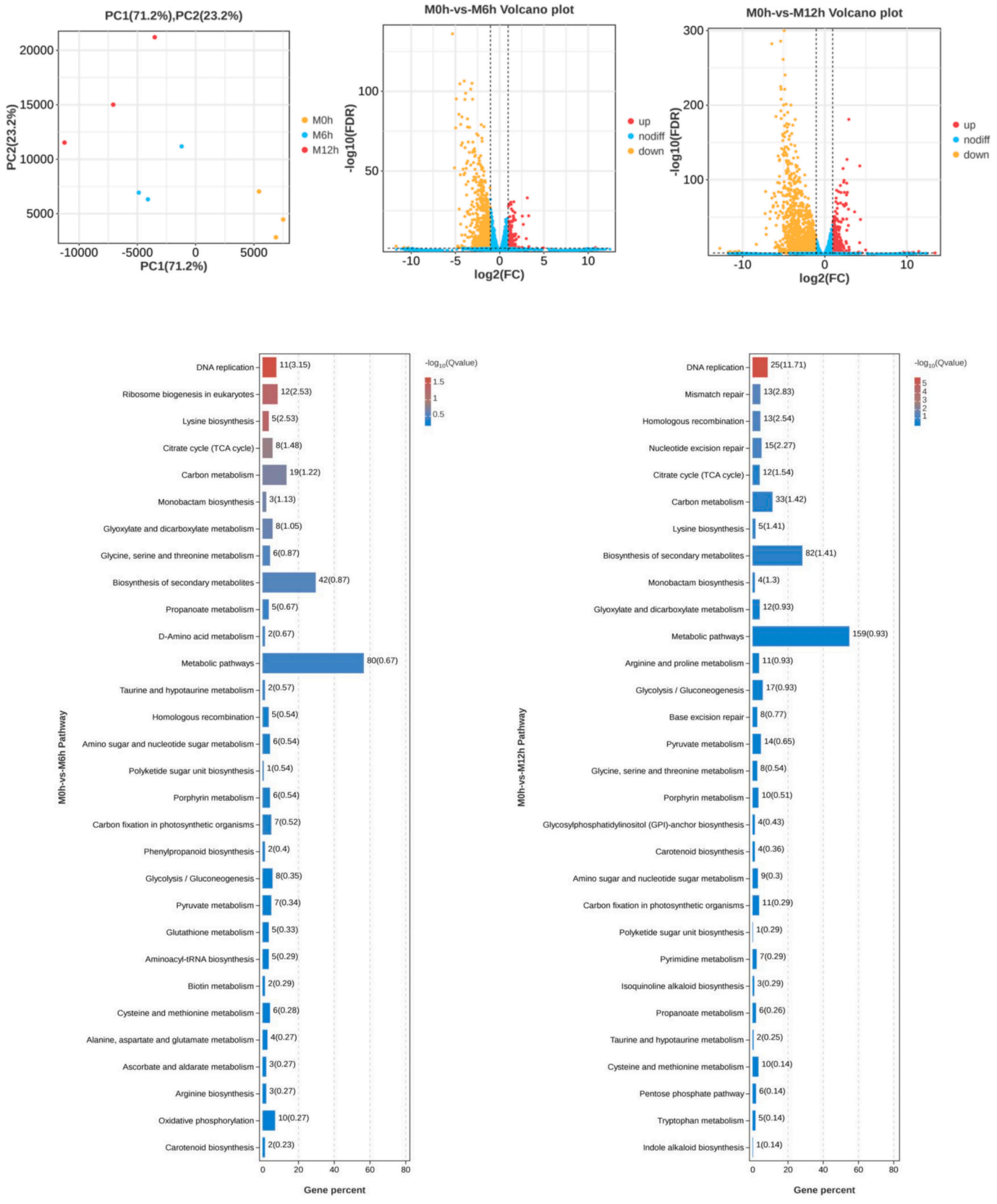

Fig. 3. Global transcriptomic profiling and differential gene expression analysis of MT03 under a C/N ratio of 16:1 at three time points following carbon depletion: M0h (onset of depletion), M6h (6 h post-depletion), and M12h (12 h post-depletion). (a) Principal component analysis (PCA) score plot illustrating transcriptional divergence across time points; (b) Volcano plot depicting differentially expressed genes (DEGs) between M0h and M6h; (c) Volcano plot showing DEGs between M0h and M12h; (d) KEGG pathway enrichment analysis of DEGs identified in the M0h vs. M6h comparison; (e) KEGG pathway enrichment analysis of DEGs identified in the M0h vs. M12h comparison.

markedly, with 485 genes upregulated and 1596 genes downregulated (Fig. 3(c)). KEGG pathway enrichment analysis of these DEGs (Fig. 3(d) and (e)) showed significant overrepresentation of pathways associated with carbon metabolism, porphyrin metabolism, carotenoid biosynthesis, and several amino acid metabolic pathways. These enriched pathways are consistent with the observed biochemical composition in MT03 (Fig. 2), including the concurrent increases in lutein and protein contents during carbon depletion, thereby providing a transcriptional basis for the strain's metabolic adaptation under nutrient stress.

3.3.1. Time-course analysis of gene expression related to carbon and nitrogen metabolism

Given the significant alterations in carbon metabolism and the biosynthesis of specific amino acids observed in MT03 (Table 1), a comprehensive analysis of gene expression related to carbon and nitrogen metabolism was performed. In heterotrophic cultivation, microalgal cells utilize glucose as their sole carbon source, which is catabolized through glycolysis to acetyl-CoA for entry into the tricarboxylic acid (TCA) cycle. As illustrated in Fig. 4, key TCA cycle–associated genes, including *OGDH*, *SUCS*, *SDH*, and *MDH*, were significantly downregulated over time following carbon depletion, indicating pronounced suppression of TCA cycle activity under carbon-limited conditions. Since the TCA cycle provides essential carbon skeletons and energy in the form of ATP and NAD(*P*)H to sustain cellular growth, the decline in biomass concentration observed after carbon depletion (Fig. 1) is likely a direct consequence of this metabolic repression.

Concurrently, the expression of *ALT* (alanine transaminase) exhibited a progressive upregulation over time, promoting the transamination of pyruvate and thereby enhancing the biosynthesis of alanine and other related amino acids. In contrast, *GDHA* (glutamate dehydrogenase (NADP+)) was progressively downregulated, which would limit the deamination of glutamate to 2-oxoglutarate and help preserve intracellular glutamate pools. These transcriptional changes align with the elevated intracellular concentrations of alanine and glutamate measured at 6 h (M6h) and 12 h (M12h) post-carbon depletion (Table 1). A positive correlation between *ALT* expression and amino acid accumulation has also been documented in *Chlorella* species [38], further supporting the functional relevance of this regulatory pattern.

Acetyl-CoA is a central metabolic node, feeding into both the fatty acid biosynthesis and TCA cycle. The conversion of acetyl-CoA to malonyl-CoA is catalyzed by acetyl-CoA carboxylase (ACC), the first committed and rate-limiting enzyme in fatty acid biosynthesis, providing the essential substrate for chain elongation [39]. It was found that the expression levels of *ACC* and *OASIII* in MT03 were significantly upregulated at both M6h and M12h, which likely promotes fatty acid biosynthesis. This transcriptional response aligns with the observed increase in lipid content (Fig. 2(c)). Similarly, in a study on *Chlamydomonas reinhardtii* CW-15, overexpression of *ACC* was shown to directly enhance lipid accumulation [40].

Starch biosynthesis proceeds from glucose-6-phosphate (G6P) via glucose-1-phosphate (G1P) and ADP-glucose to amylose formation. As illustrated in Fig. 4, the expression of *GBSS* (granule-bound starch synthase), a central gene in starch biosynthesis, was markedly downregulated over time in MT03. In contrast, the starch-degrading gene *ISA* (isoamylase) was significantly upregulated at M6h and M12h. A previous study has demonstrated a strong negative correlation between *ISA* expression and starch content [41]. Collectively, the reduction in total carbohydrate content in MT03 (Fig. 2(d)) appears to stem from suppressed starch biosynthesis and enhanced starch degradation at the transcriptional level following carbon depletion. This mechanism may help the microalgal cells to survive from glucose starvation, resulting in a relatively stable biomass concentration after an initial decline (Fig. 1).

3.3.2. Time-course analysis of gene expression related to pigment metabolism

Given the substantial difference in lutein content in MT03 before and after carbon depletion, the expression profiles of genes involved in porphyrin and carotenoid biosynthesis were analyzed. Porphyrin metabolism originates from L-glutamate and proceeds through a series of enzymatic reactions to form protoporphyrin IX, which serves as the common branch-point precursor for both heme and chlorophyll biosynthesis [42]. A previous study has shown that in MT03, a G1106D substitution in the CHLH subunit of magnesium chelatase impairs magnesium insertion into PIX, resulting in loss of enzyme activity and consequent blockade of metabolic flux into the chlorophyll branch [24]. As shown in Fig. 5, genes associated with protoporphyrin IX biosynthesis, such as *HMBS* and *UROD*, exhibited a progressive downregulation over time. In contrast, heme content was significantly higher at both M6h and M12h compared to M0h. This accumulation may be attributed to the pronounced downregulation of heme degradation–related genes during the post-depletion phase (Fig. 5). Moreover, despite an overall reduction in porphyrin pathway flux, the obstruction of chlorophyll synthesis is expected to shunt a greater proportion of the available PIX toward heme biosynthesis. Heme functions as an essential cofactor for cytochrome P450 enzymes (e.g., CYP97s), mediating electron transfer from NADPH to molecular oxygen; thus, its cellular availability can directly modulate the catalytic efficiency of CYP97s in lutein biosynthesis [43]. The observed suppression of heme degradation genes likely promoted heme accumulation, thereby enhancing the enzymatic capacity of CYP97s to catalyze the conversion of α-carotene to lutein.

In the carotenoid biosynthetic pathway, which originates from the terpenoid backbone, phytoene is sequentially desaturated by phytoene desaturase (PDS) to ζ-carotene and then by ζ-carotene desaturase (ZDS) to lycopene [44]. As illustrated in Fig. 5, *PDS* and *ZDS* showed significant upregulation at M6h and M12h, potentially increasing lycopene availability and thereby promoting downstream carotenoid biosynthesis. Previous studies have reported that *PDS* expression is strongly upregulated during carotenoid accumulation in *Haematococcus pluvialis* [45], and that endogenous overexpression of *PDS* significantly enhances carotenoid production [46]. Lycopene is subsequently channeled into two major branches. One branch involves the conversion of lycopene to δ-carotene, followed by cyclization catalyzed by lycopene β-cyclase (LCYB) to form α-carotene [47]. α-Carotene is then hydroxylated by CYP97C or CYP97A to yield α-cryptoxanthin or zeinoxanthin, respectively, which are ultimately converted to lutein [48]. In this study, the

Table 1
Amino acid composition of the MT03 strain at three time points: glucose depletion (M0h), 6 h post-depletion (M6h), and 12 h post-depletion (M12h). Data marked with asterisks indicate significant differences between M6h/M12h and M0h as determined by two-tailed *t*-tests (*$p < 0.05$, **$p < 0.01$).

Amino acids (AA, %DW)		M0h	M6h	M12h
Essential amino acids (EAAs)	Lys	2.34 ± 0.05	2.81 ± 0.14**	2.97 ± 0.09**
	Phe	0.88 ± 0.03	1.11 ± 0.03**	1.18 ± 0.03**
	Thr	1.17 ± 0.02	1.40 ± 0.08**	1.47 ± 0.04**
	Met	0.52 ± 0.02	0.46 ± 0.19	0.65 ± 0.02**
	Ile	0.64 ± 0.03	0.86 ± 0.06**	0.91 ± 0.02**
	Leu	1.77 ± 0.04	2.30 ± 0.11**	2.41 ± 0.07**
	Val	1.11 ± 0.05	1.29 ± 0.11	1.38 ± 0.04**
	Arg	2.28 ± 0.01	2.27 ± 0.19	2.36 ± 0.02**
	His	0.55 ± 0.01	0.60 ± 0.06	0.64 ± 0.05*
Non-essential amino acids (NEEAs)	Gly	1.27 ± 0.03	1.40 ± 0.13	1.51 ± 0.04**
	Ala	1.89 ± 0.04	2.14 ± 0.26**	2.33 ± 0.05**
	Asp	2.31 ± 0.07	2.55 ± 0.12*	2.66 ± 0.04**
	Ser	1.12 ± 0.04	1.25 ± 0.10	1.33 ± 0.03**
	Glu	3.60 ± 0.03	4.84 ± 0.45**	5.34 ± 0.34**
	Pro	1.39 ± 0.09	1.42 ± 0.01	1.43 ± 0.06
	Cys	0.00 ± 0.00	0.23 ± 0.06**	0.32 ± 0.01**
	Tyr	1.88 ± 0.03	2.18 ± 0.07**	2.36 ± 0.03**
Total EAAs		11.28 ± 0.23	10.22 ± 0.72*	10.97 ± 0.31
Total NEAAs		13.46 ± 0.14	18.88 ± 1.43**	20.28 ± 0.67**
Total AA		24.74 ± 0.37	29.10 ± 2.14	31.25 ± 0.98**

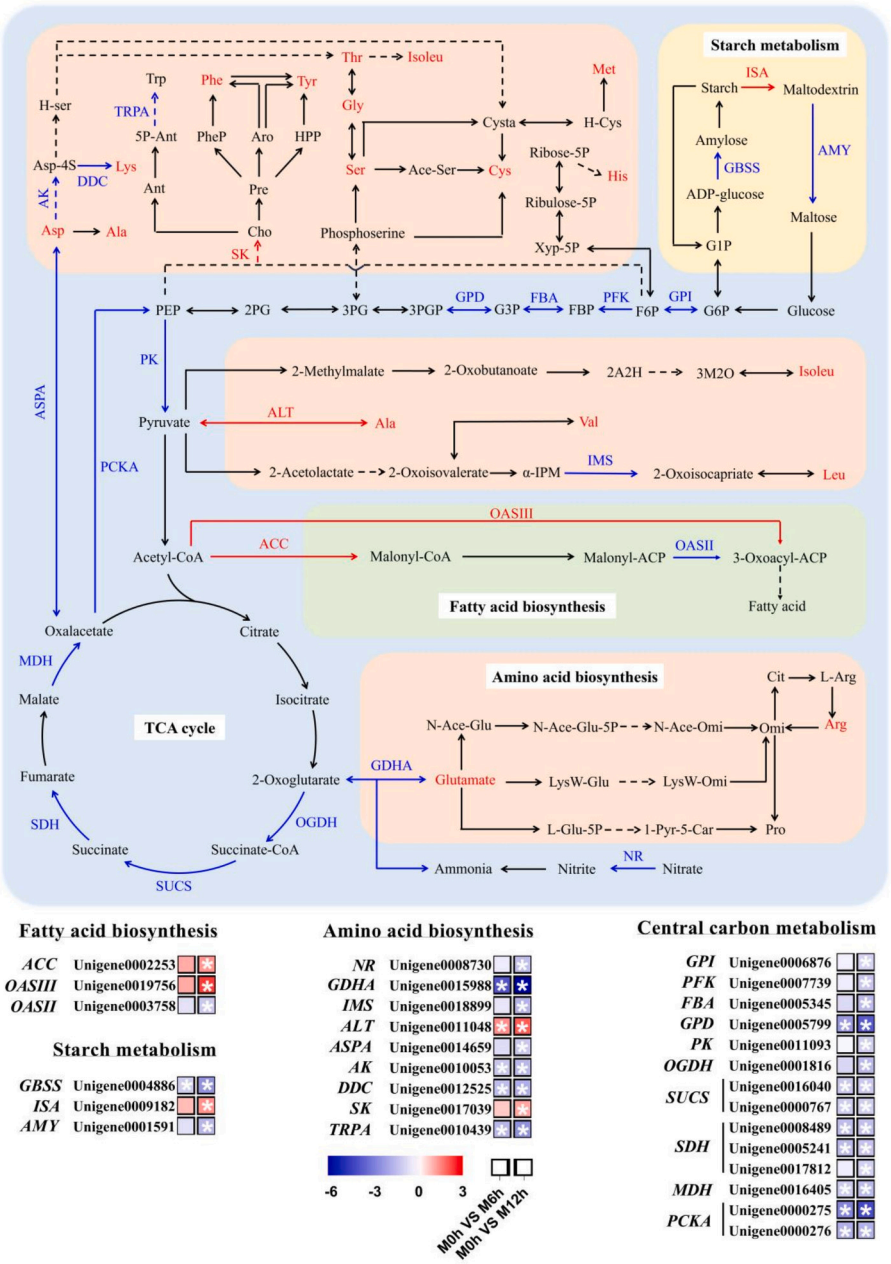

Fig. 4. Comparative analysis of gene expression profiles related to central carbon metabolism, starch metabolism, fatty acid biosynthesis, and amino acid biosynthesis in MT03 under a C/N ratio of 16:1 at three time points following carbon depletion: M0h (onset of depletion), M6h (6 h post-depletion), and M12h (12 h post-depletion). ACC: acetyl-CoA carboxylase; AK: aspartate kinase; ALT: alanine transaminase; AMY: alpha-amylase; ASAP: aspartate aminotransferase; DDC: diaminopimelate decarboxylase; FBA: fructose-bisphosphate aldolase; GBSS: granule-bound starch synthase; GDHA: glutamate dehydrogenase (NADP+); GPD: glyceraldehyde 3-phosphate dehydrogenase; GPI: glucose-6-phosphate isomerase; ISA: isoamylase; IMS: 2-isopropylmalate synthase; MDH: malate dehydrogenase; NR: nitrate reductase (NAD(*P*)H); OASII: 3-oxoacyl-[acyl-carrier-protein] synthase II; OASIII: 3-oxoacyl-[acyl-carrier-protein] synthase III; OGDH: 2-oxoglutarate dehydrogenase E1 component; PCKA: phosphoenolpyruvate carboxykinase; PFK: 6-phosphofructokinase; PK: pyruvate kinase; SDH: succinate dehydrogenase flavoprotein subunit; SK: shikimate kinase; SUCS: succinyl-CoA synthetase alpha subunit; TRPA: tryptophan synthase alpha chain. The data with asterisks indicate significant differences (FDR $<$ 0.05 and FC $\geq$ 2).

expression levels of both *LCYB* and *CYP97C* exhibited significant upregulation over time, which correlates well with the observed increase in lutein content following carbon depletion.

Collectively, the findings from these transcriptional analyses provide a mechanistic basis for the enhanced co-accumulation of lutein and protein in MT03 under carbon-depleted and nitrogen-replete conditions. This highlights the coordinated regulation of central carbon metabolism, macromolecular biosynthesis, heme homeostasis, and carotenoid biosynthesis in response to nutrient stress. The MT03 is a chlorophyll-deficient yellow mutant of *C. sorokiniana*, resulting from a mutation in the CHLH subunit of magnesium chelatase. This mutation substitutes glycine with aspartic acid at position 1106 (G1106D), which impairs the magnesium chelation reaction and consequently disrupts chlorophyll biosynthesis [24]. Hence, the mutant MT03 remains a strain of *C. sorokiniana*. The mechanistic basis for the enhanced co-accumulation of lutein and protein under carbon-depleted and nitrogen-replete conditions may be applicable to other strain of *C. sorokiniana*.

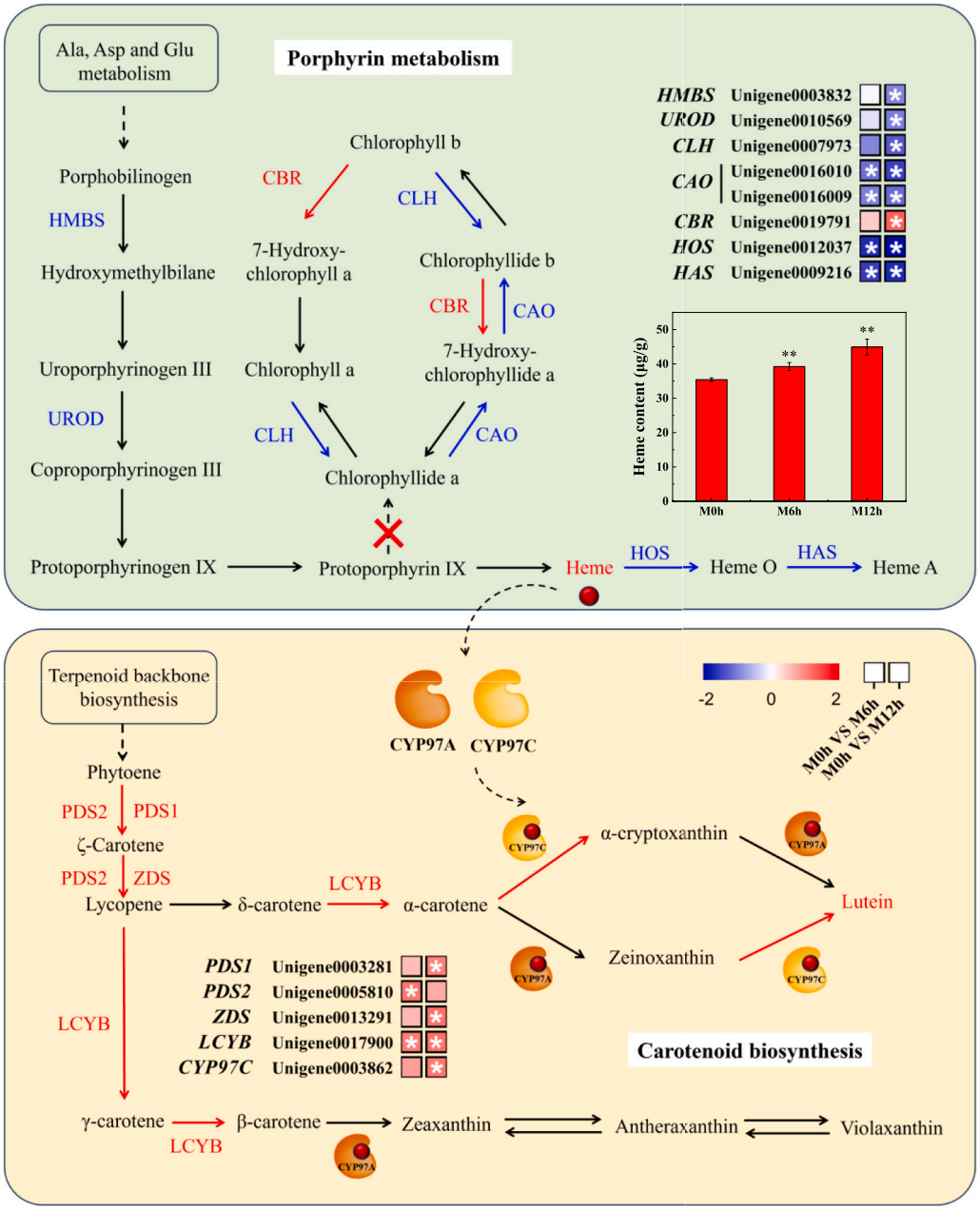

Fig. 5. Comparative analysis of gene expression profiles related to porphyrin metabolism and carotenoid biosynthesis in MT03 under a C/N ratio of 16:1 at three time points following carbon depletion: M0h (onset of depletion), M6h (6 h post-depletion), and M12h (12 h post-depletion). HMBS: hydroxymethylbilane synthase; UROD: uroporphyrinogen decarboxylase; CAO: chlorophyllide a oxygenase; CBR: chlorophyll(ide) b reductase; CLH: chlorophyllase I; CYP97C: carotenoid epsilon hydroxylase; HAS: heme a synthase; HOX: heme o synthase; LCYB: lycopene beta-cyclase; PDS1: 15-cis-phytoene desaturase; PDS2: phytoene desaturase (3,4-didehydrolycopene-forming); ZDS: zeta-carotene desaturase. The data with asterisks indicate significant differences (FDR < 0.05 and FC ≥ 2).

3.4. Enhancing lutein and protein co-production through carbon–nitrogen metabolic regulation in a 5-L bioreactor

The aforementioned results indicate that a C/N ratio of 16:1 represents the optimal condition for the co-production of lutein and protein in MT03. Although further induction under carbon-depleted and nitrogen-replete conditions is detrimental to cell growth, it markedly enhances the cellular contents of both lutein and protein. To validate the efficacy of this two-stage strategy, MT03 was cultivated in a 5-L bioreactor. By day 2, residual glucose in the broth declined to around 5 g/L (Fig. 6(a)). Thereafter, glucose was maintained at ~5 g/L through fed-batch addition of a 22.85-fold concentrated medium (C/N ratio: 16:1) via a peristaltic pump. Concurrently, the urea concentration in the broth initially decreased, followed by a slight increase before stabilizing, suggesting that nitrogen demand varies across different growth phases. Under this feeding regime, MT03 achieved a biomass concentration of 209.88 g/L after 7.5 days of cultivation. Despite the high cell density, the fermentation broth remained well-mixed and exhibited good fluidity throughout the cultivation, with algal cells uniformly dispersed in the bioreactor without sedimentation or paste formation. This homogeneous suspension was maintained through appropriate agitation and aeration, enabling stable process performance even at such elevated biomass levels. This performance is consistent with a previous report demonstrating that *C. sorokiniana* CMBB276 can achieve ultrahigh-cell-

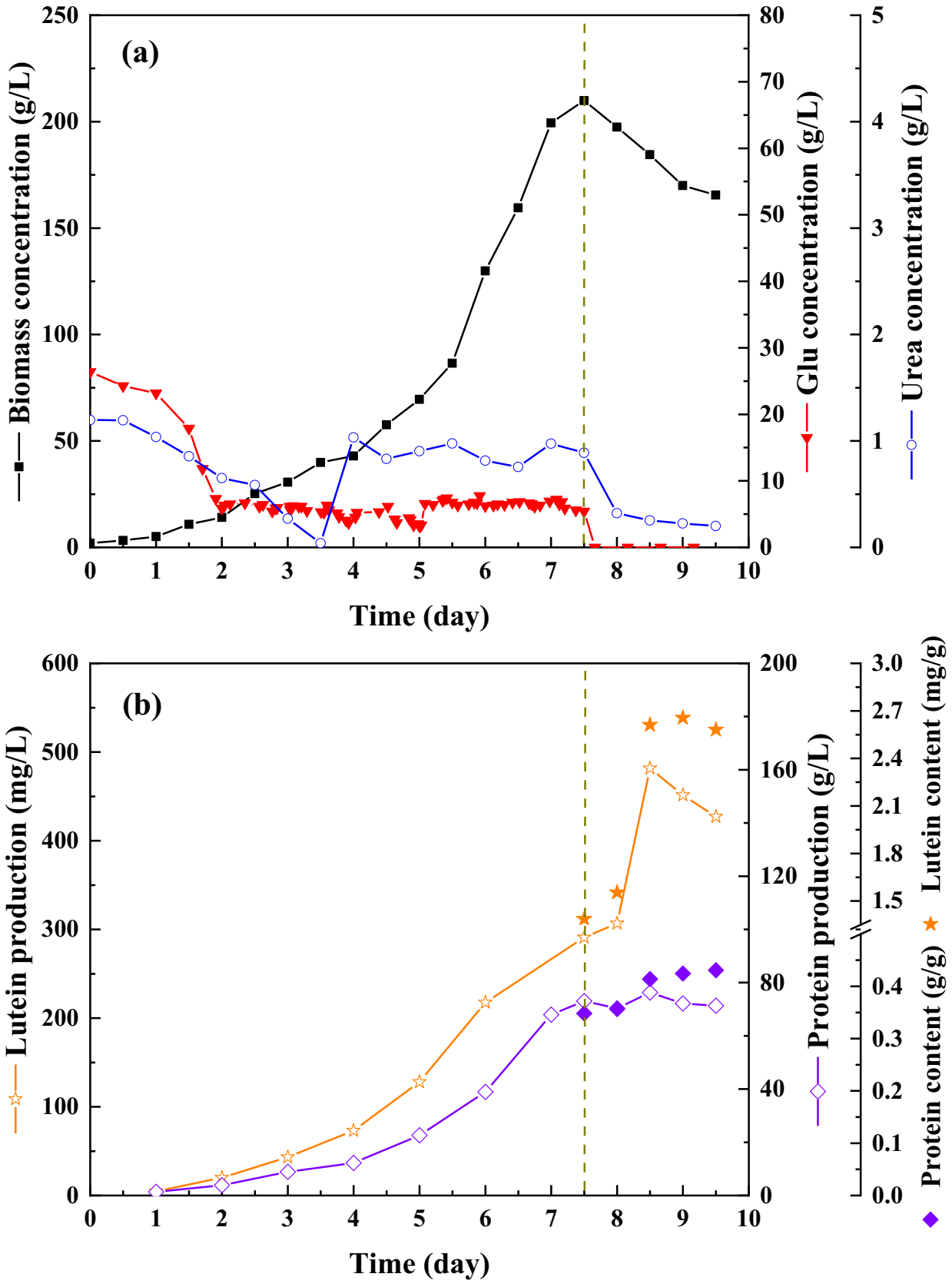

Fig. 6. Time-course profiles of (a) cell growth and nutrient consumption, and (b) lutein and protein production by MT03 cultivated in a 5-L bioreactor. The dashed vertical line denotes the time point at which fed-batch feeding was terminated to induce carbon-depleted and nitrogen-replete conditions.

density cultivation (>200 g/L biomass within 6 days) when a stepwise constant feeding approach is employed to maintain glucose concentrations in the 5–10 g/L range [11].

However, at this stage, the cellular contents of lutein and protein remained relatively low at 1.39 mg/g and 0.35 g/g, respectively (Fig. 6 (b)). To further enhance product accumulation, feeding was terminated at 7.5 days to establish carbon-depleted and nitrogen-replete conditions. As illustrated in Fig. 6(a), glucose was rapidly exhausted to 0 g/L following feed cessation, while urea concentration dropped sharply to ~0.32 g/L and then gradually declined to ~0.20 g/L by day 9.5. Correspondingly, biomass concentration decreased significantly due to carbon limitation, falling to 165.52 g/L by day 9.5. Notably, however, lutein and protein contents increased dramatically within 24 h, by 87.8% and 17.1%, respectively, reaching values of 2.61 mg/g and 0.41 g/g at day 8.5, after which they remained relatively stable (Fig. 6(b)). These findings demonstrate that while a C/N ratio of 16:1 supports maximal biomass accumulation, a subsequent shift to carbon-depleted and nitrogen-replete conditions effectively triggers metabolic reprogramming that favors the co-accumulation of lutein and protein, despite a trade-off in biomass yield. Additionally, urea was employed as the nitrogen source in the bioreactor to circumvent the inhibitory effect of sodium ion accumulation associated with sodium nitrate use [11]. This choice resulted in a substantially lower lutein content compared to shake-flask cultures using sodium nitrate (4.34 mg/g) (Fig. 2(a)). Similarly, a previous study has reported that lutein accumulation in *C. sorokiniana* FZU60 is significantly higher under sodium nitrate than under urea [12].

Under the implemented two-stage strategy, MT03 achieved maximum production of 481.63 mg/L for lutein and 76.31 g/L for protein (Fig. 6(b)). To the best of current knowledge, lutein production reported in microalgal systems typically ranges from 14.8 to 415.93 mg/L [1,2,12,49,50]. Thus, the lutein production attained in this study represents the highest value documented to date. In comparison, protein production in microalgae has also been enhanced through advanced heterotrophic processes. For instance, an ultrahigh-density cultivation of the high-protein strain *C. sorokiniana* CMBB276, employing pH control via ammonium hydroxide and reduced nitrogen feeding, yielded 86.55 g/L protein with a cellular content of 37.3% [11]. More recently, reducing the C/N ratio from 18 to 6 via a two-stage nitrogen modulation approach further increased protein content to 58.6% and achieved a final titer of 87.0 g/L [26]. Although the protein production in MT03 is marginally lower than these values, it exceeds the majority of previously reported titers, which typically range from 4.15 to 16.76 g/L [25,51,52]. Notably, the chlorophyll-deficient phenotype of MT03 is inherently linked to constitutively elevated lutein and protein levels, highlighting its strong potential for the industrial-scale co-production of these high-value biomolecules.

4. Conclusions

Strategic modulation of carbon–nitrogen metabolism through C/N ratio adjustment effectively enhances lutein and protein biosynthesis in heterotrophically cultivated *C. sorokiniana* MT03. Integrated physiological and transcriptomic analyses demonstrate that carbon depletion coupled with nitrogen repletion redirected metabolic flux toward lutein and protein synthesis while suppressing competing pathways. Successful scale-up using a two-stage strategy (i.e., Stage I for high-density biomass accumulation and Stage II for lutein and protein induction) in a 5-L bioreactor yielded 184.46 g/L biomass, 415.93 mg/L lutein, and 76.31 g/L protein. This work provides a robust and scalable solution to the primary bottleneck limiting commercial production of microalgal lutein and protein.

CRediT authorship contribution statement

Yucheng Chen: Writing – original draft, Validation, Conceptualization. **Zehao Qiu:** Methodology, Investigation, Data curation. **Wen Zhang:** Methodology, Investigation, Data curation. **Xinxin Huang:** Methodology, Investigation, Data curation. **Ruijuan Ma:** Writing – review & editing, Visualization, Validation, Conceptualization. **Baobei Wang:** Methodology, Conceptualization. **Shih-Hsin Ho:** Writing – review & editing, Conceptualization. **Jianfeng Chen:** Resources. **Youping Xie:** Writing – review & editing, Validation, Supervision, Conceptualization.

Declaration of competing interest

The authors declare that they have no known competing financial interests or personal relationships that could have appeared to influence the work reported in this paper.

Acknowledgments

This study was financially supported by the Natural Science Foundation of Fujian Province, China (No. 2024J09039), the National Natural Science Foundation of China (No. 32202960), the Fujian College Association Instrumental Analysis Center of Fuzhou University Testing Fund of Precious Apparatus (2026T044), and the Fuzhou University Research Start-up Fund (XRC-25153).

Appendix A. Supplementary data

Supplementary data to this article can be found online at https://doi.org/10.1016/j.algal.2026.104626.

Data availability

Data will be made available on request.

References

[1] M.S. Kadri, R.R. Singhania, G.S. Anisha, N. Gohil, V. Singh, A.K. Patel, A.K. Patel, Microalgal lutein: advancements in production, extraction, market potential, and applications, Bioresour. Technol. 389 (2023) 129808.
[2] C. Camarena-Bernard, V. Pozzobon, Evolving perspectives on lutein production from microalgae - a focus on productivity and heterotrophic culture, Biotechnol. Adv. 73 (2024) 108375.
[3] H. Bartlett, O. Howells, F. Eperjesi, The role of macular pigment assessment in clinical practice: a review, Clin. Exp. Optom. 93 (2010) 300–308.
[4] Q. Bian, P. Zhou, Z. Yao, M. Li, H. Yu, L. Ye, Heterologous biosynthesis of lutein in S. cerevisiae enabled by temporospatial pathway control, Metab. Eng. 67 (2021) 19–28.
[5] Z. Qin, M. Liu, X. Ren, W. Zeng, Z. Luo, J. Zhou, De novo biosynthesis of lutein in *Yarrowia lipolytica*, J. Agric. Food Chem. 72 (2024) 5348–5357.
[6] Y. Xie, X. Xiong, S. Chen, Challenges and potential in increasing lutein content in microalgae, Microorganisms 9 (2021) 1068.
[7] H. Goshtasbi, Y.B. Okolodkov, A. Movafeghi, S. Awale, A. Safary, J. Barar, Y. Omidi, Harnessing microalgae as sustainable cellular factories for biopharmaceutical production, Algal Res. 74 (2023) 103237.
[8] J.A. Garrido-Cardenas, F. Manzano-Agugliaro, F.G. Acien-Fernandez, E. Molina-Grima, Microalgae research worldwide, Algal Res. 35 (2018) 50–60.
[9] Y. Torres-Tiji, F.J. Fields, S.P. Mayfield, Microalgae as a future food source, Biotechnol. Adv. 41 (2020) 107536.
[10] H. Jin, W. Chuai, K. Li, G. Hou, M. Wu, J. Chen, H. Wang, J. Jia, D. Han, Q. Hu, Ultrahigh-cell-density heterotrophic cultivation of the unicellular green alga *Chlorella sorokiniana* for biomass production, Biotechnol. Bioeng. 118 (2021) 4138–4151.
[11] Q. Xu, G. Hou, J. Chen, H. Wang, L. Yuan, D. Han, Q. Hu, H. Jin, Heterotrophically ultrahigh-cell-density cultivation of a high protein-yielding unicellular alga *Chlorella* with a novel nitrogen-supply strategy, Front. Bioeng. Biotechnol. 9 (2021) 774854.
[12] Y. Xie, Z. Zhang, R. Ma, X. Liu, M. Miao, S.H. Ho, J. Chen, Y.K. Leong, J.S. Chang, High-cell-density heterotrophic cultivation of microalga *Chlorella sorokiniana* FZU60 for achieving ultra-high lutein production efficiency, Bioresour. Technol. 365 (2022) 128130.
[13] X. Zhao, J. Yan, T. Yang, P. Xiong, X. Zheng, Y. Lu, K. Jing, Exploring engineering reduced graphene oxide-titanium dioxide (RGO-TiO2) nanoparticles treatment to effectively enhance lutein biosynthesis with *Chlorella sorokiniana* F31 under different light intensity, Bioresour. Technol. 348 (2022) 126816.

[14] A.K. Patel, A.P. Vadrale, R.-R. Singhania, C.-W. Chen, J.S. Chang, C.-D. Dong, Enhanced mixotrophic production of lutein and lipid from potential microalgae isolate *Chlorella sorokiniana* C16, Bioresour. Technol. 386 (2023) 129477.
[15] J.H. Chen, Y. Kato, M. Matsuda, C.Y. Chen, D. Nagarajan, T. Hasunuma, A. Kondo, J.S. Chang, Lutein production with *Chlorella sorokiniana* MB-1-M12 using novel two-stage cultivation strategies – metabolic analysis and process improvement, Bioresour. Technol. 334 (2021) 125200.
[16] A.P. Vadrale, C.-D. Dong, D. Haldar, C.-H. Wu, C.-W. Chen, R.R. Singhania, A. K. Patel, Bioprocess development to enhance biomass and lutein production from *Chlorella sorokiniana* Kh12, Bioresour. Technol. 370 (2023) 128583.
[17] A.K. Patel, A.P. Vadrale, Y.S. Tseng, C.W. Chen, C.D. Dong, R.R. Singhania, Bioprospecting of marine microalgae from Kaohsiung Seacoast for lutein and lipid production, Bioresour. Technol. 351 (2022) 126928.
[18] C.V. Do, C.T. Dinh, M.T. Dang, T.D. Tran, T.G. Le, A novel flat-panel photobioreactor for simultaneous production of lutein and carbon sequestration by *Chlorella sorokiniana* TH01, Bioresour. Technol. 345 (2022) 126552.
[19] C.Y. Chen, I.C. Lu, D. Nagarajan, C.H. Chang, I.S. Ng, D.J. Lee, J.S. Chang, A highly efficient two-stage cultivation strategy for lutein production using heterotrophic culture of *Chlorella sorokiniana* MB-1-M12, Bioresour. Technol. 253 (2018) 141–147.
[20] U. Kim, D.H. Cho, J. Heo, J.H. Yun, D.Y. Choi, K. Cho, H.S. Kim, Two-stage cultivation strategy for the improvement of pigment productivity from high-density heterotrophic algal cultures, Bioresour. Technol. 302 (2020) 122840.
[21] C. Zhang, H. Liu, Y. Zong, Z. Tu, H. Li, Isolation, expression, and functional analysis of the geranylgeranyl pyrophosphate synthase (GGPPS) gene from *Liriodendron tulipifera*, Plant Physiol. Biochem. 166 (2021) 700–711.
[22] H. Qing, J. Chen, L. Jiang, J. Qian, J. Fu, C. Zhang, Functional characterization of two lycopene cyclases from sweet osmanthus (*Osmanthus fragrans*), Sci. Hortic. 299 (2022) 111062.
[23] T. Fabryova, D. Kubac, M. Kuzma, P. Hrouzek, J. Kopecky, L. Tumova, J. Cheel, High-performance countercurrent chromatography for lutein production from a chlorophyll-deficient strain of the microalgae *Parachlorella kessleri* HY1, J. Appl. Phycol. 33 (2021) 1999–2013.
[24] Y. Xie, W. Lin, W. Zhang, X. Meng, R. Ma, B. Wang, S.-H. Ho, J. Chen, J.-S. Chang, Chlorophyll-deficient triggers heterotrophic lutein-directed biosynthesis in a novel mutant strain of *Chlorella sorokiniana* (Chlorophyta): Process characterization and underlying mechanism, Aquaculture 598 (2025) 741998.
[25] X. Xiao, Y. Zhou, Z. Liang, R. Lin, M. Zheng, B. Chen, Y. He, A novel two-stage heterotrophic cultivation for starch-to-protein switch to efficiently enhance protein content of *Chlorella* sp. MBFJNU-17, Bioresour. Technol. 344 (2022) 126187.
[26] B. Chen, R. Gong, Z. Qiao, J. Men, L. Tan, S. Tian, H. Jin, Improving *Chlorella* protein production under heterotrophic high cell density fed-batch cultivation with a two-stage nitrogen nutrient supply strategy, Green Carbon 3 (2025) 208–217.
[27] R. Ma, Z. Zhang, S.-H. Ho, C. Ruan, J. Li, Y. Xie, X. Shi, L. Liu, J. Chen, Two-stage bioprocess for hyper-production of lutein from microalga *Chlorella sorokiniana* FZU60: Effects of temperature, light intensity, and operation strategies, Algal Res. 52 (2020) 102119.
[28] R. Ma, X. Zhao, S.-H. Ho, X. Shi, L. Liu, Y. Xie, J. Chen, Y. Lu, Co-production of lutein and fatty acid in microalga *Chlamydomonas* sp. JSC4 in response to different temperatures with gene expression profiles, Algal Res. 47 (2020) 101821.
[29] C.-H. Su, R. Giridhar, C.-W. Chen, W.-T. Wu, A novel approach for medium formulation for growth of a microalga using motile intensity, Bioresour. Technol. 98 (2007) 3012–3016.
[30] R. Ma, Z. Zhang, Z. Tang, S.-H. Ho, X. Shi, L. Liu, Y. Xie, J. Chen, Enhancement of co-production of lutein and protein in *Chlorella sorokiniana* FZU60 using different bioprocess operation strategies, Bioresour. Bioprocess. 8 (2021) 82.
[31] M. Liu, W. Ma, X. Su, X. Zhang, Y. Lu, S. Zhang, J. Yan, D. Feng, L. Ma, A. Taylor, Y. Ge, Q. Cheng, K. Xu, Y. Wang, N. Li, A. Gu, J. Zhang, S. Luo, S. Xuan, X. Chen, N. S. Scrutton, C. Li, J. Zhao, S. Shen, Mutation in a chlorophyll- binding motif of *Brassica* ferrochelatase enhances both heme and chlorophyll biosynthesis, Cell Rep. 41 (2022) 111758.
[32] R. Ma, Z. Zhang, H. Fang, X. Liu, S.-H. Ho, Y. Xie, J. Chen, Unveiling the underlying molecular mechanisms of high lutein production efficiency in *Chlorella sorokiniana* FZU60 under a mixotrophy/photoautotrophy two-stage strategy by transcriptomic, physiological, and biochemical analyses, Biotechnol. Biofuels Bioprod. 16 (2023) 47.
[33] M.I. Love, W. Huber, S. Anders, Moderated estimation of fold change and dispersion for RNA-seq data with DESeq2, Genome Biol. 15 (2014) 550.
[34] M.D. Robinson, D.J. McCarthy, G.K. Smyth, edgeR: a Bioconductor package for differential expression analysis of digital gene expression data, Bioinformatics 26 (2010) 139–140.
[35] S.H. Ho, A. Nakanishi, X.T. Ye, J.S. Chang, C.Y. Chen, T. Hasunuma, A. Kondo, Dynamic metabolic profiling of the marine microalga *Chlamydomonas* sp. JSC4 and enhancing its oil production by optimizing light intensity, Biotechnol. Biofuels 8 (2015) 48.
[36] S. Vyas, A. Patel, E. Nabil Risse, E. Krikigianni, U. Rova, P. Christakopoulos, L. Matsakas, Biosynthesis of microalgal lipids, proteins, lutein, and carbohydrates using fish farming wastewater and forest biomass under photoautotrophic and heterotrophic cultivation, Bioresour. Technol. 359 (2022) 127494.
[37] T. Li, Y. Zheng, L. Yu, S. Chen, High productivity cultivation of a heat-resistant microalga *Chlorella sorokiniana* for biofuel production, Bioresour. Technol. 131 (2013) 60–67.
[38] H. Chen, Y. Zheng, J. Zhan, C. He, Q. Wang, Comparative metabolic profiling of the lipid-producing green microalga *Chlorella* reveals that nitrogen and carbon metabolic pathways contribute to lipid metabolism, Biotechnol. Biofuels 10 (2017) 153.
[39] Y. Li-Beisson, J.J. Thelen, E. Fedosejevs, J.L. Harwood, The lipid biochemistry of eukaryotic algae, Prog. Lipid Res. 74 (2019) 31–68.
[40] D. Chen, X. Yuan, L.M. Liang, K. Liu, H.Y. Ye, Z.Y. Liu, Y.F. Liu, L.Q. Huang, W. J. He, Y.Q. Chen, Y.D. Zhang, T. Xue, Overexpression of acetyl-CoA carboxylase increases fatty acid production in the green alga *Chlamydomonas reinhardtii*, Biotechnol. Lett. 41 (2019) 1133–1145.
[41] C.C. Guo, J.G. Li, M.H. Li, X.H. Xu, Y. Chen, J.Z. Chu, X.Q. Yao, Regulation mechanism of exogenous brassinolide on bulbil formation and development in *Pinellia ternata*, Front. Plant Sci. 12 (2022) 809769.
[42] T. Fan, L. Roling, B. Hedtke, B. Grimm, FC2 stabilizes POR and suppresses ALA formation in the tetrapyrrole biosynthesis pathway, New Phytol. 239 (2023) 624–638.
[43] S.Y. Park, H. Eun, M.H. Lee, S.Y. Lee, Metabolic engineering of *Escherichia coli* with electron channelling for the production of natural products, Nat. Catal. 5 (2022) 726–737.
[44] M. Li, Z. Gan, Y. Cui, C. Shi, X. Shi, Structure and function characterization of the phytoene desaturase related to the lutein biosynthesis in *Chlorella protothecoides* CS-41, Mol. Biol. Rep. 40 (2013) 3351–3361.
[45] K. Grünewald, M. Eckert, J. Hirschberg, C. Hagen, Phytoene desaturase is localized exclusively in the chloroplast and up-regulated at the mRNA level during accumulation of secondary carotenoids in *Haematococcus pluvialis* (Volvocales, Chlorophyceae), Plant Physiol. 122 (2000) 1261–1268.
[46] J.I. Galarza, J.A. Gimpel, V. Rojas, B.O. Arredondo-Vega, V. Henriquez, Over-accumulation of astaxanthin in *Haematococcus pluvialis* through chloroplast genetic engineering, Algal Res. 31 (2018) 291–297.
[47] H. Fang, J. Liu, R. Ma, Y. Zou, S.H. Ho, J. Chen, Y. Xie, Functional characterization of lycopene β- and ε-cyclases from a lutein-enriched green microalga *Chlorella sorokiniana* FZU60, Mar. Drugs 21 (2023) 418.
[48] M.H. Liang, H. Xie, H.H. Chen, Z.C. Liang, J.G. Jiang, Functional identification of two types of carotene hydroxylases from the green alga *Dunaliella bardawil* rich in lutein, ACS Synth. Biol. 9 (2020) 1246–1253.
[49] H. Zheng, Y. Wang, S. Li, D. Nagarajan, S. Varjani, D.J. Lee, J.S. Chang, Recent advances in lutein production from microalgae, Renew. Sust. Energ. Rev. 153 (2022) 111795.
[50] J. Hu, D. Nagarajan, Q. Zhang, J.S. Chang, D.J. Lee, Heterotrophic cultivation of microalgae for pigment production: A review, Biotechnol. Adv. 36 (2018) 54–67.
[51] X. Shi, Q. Li, X. Chen, J. Xie, D. Wei, Enhanced lutein and protein production with improved organoleptic properties in a novel yellow strain of *Auxenochlorella pyrenoidosa* mutant through atmospheric and room temperature plasma mutagenesis and norflurazon-based screening, Food Res. Int. 197 (2024) 115288.
[52] B. Wang, B. Liu, Y. Li, X. Yang, D. Wei, Texture, flavor and digestibility improvement of high-moisture-extruded meat analogues by incorporating golden biomass of *Auxenochlorella pyrenoidosa* mutant through auto-controlled fermentation, Bioresour. Technol. 432 (2025) 132684.